

## Effects of metal oxide coatings on the thermal stability and electrical performance of $\text{LiCoO}_2$ in a Li-ion cell

Ho-Jin Kweon\*, JeonJoon Park, JunWon Seo, GeunBae Kim, BokHwan Jung, Hong S. Lim

Corporate R&D Center, Samsung SDI Co. Ltd., Giheung 449-902, South Korea

Received 15 July 2003; accepted 28 August 2003

### Abstract

A study is made of the effects of  $\text{MgO}$  and  $\text{Al}_2\text{O}_3$  coatings on the electrical properties of  $\text{LiCoO}_2$  cathode material on the thermal stability (differential scanning calorimetry (DSC)) of the charged cathode, and on the safety characteristics of 18650 Li-ion cells. Powdery active material is coated with Mg or Al alkoxide solutions followed by heat treatment in air at temperatures between 300 and 800 °C. The presence of the coating is confirmed by an elemental depth-profile analysis of the powder surface using secondary ion mass spectroscopy (SIMS) and X-ray photoelectron spectroscopy (XPS). Both oxide coatings, especially the  $\text{Al}_2\text{O}_3$  coating, substantially improve the charge–discharge voltage characteristics, rate capability, capacity and rate-capability retention on cycling and thermal stability of the  $\text{LiCoO}_2$  cathode. These beneficial effects are demonstrated in 18650 Li-ion cells.

© 2003 Elsevier B.V. All rights reserved.

**Keywords:**  $\text{Al}_2\text{O}_3$  coating; Li-ion battery; Cycle-life; Rate capability; Safety;  $\text{MgO}$  coating

### 1. Introduction

The cathode material is known to exert a major influence on the performance of a Li-ion cell, such as specific energy, cycle-life, rate capability and safety aspects.  $\text{LiCoO}_2$  is used almost exclusively in commercial Li-ion cells despite the fact that there are other candidate materials, namely,  $\text{LiNi}_{1-x}\text{M}_x\text{O}_2$  (where  $x = 0-1$  and M is a transition metal such as Co, Mn, etc.) and  $\text{LiMn}_2\text{O}_4$ . This is because the alternative materials have serious drawbacks. Most of the nickel-base materials are not free of safety-related concerns and high reactivity with the electrolyte in the charged state [1]. The main concern of the  $\text{LiMn}_2\text{O}_4$  spinel material is manganese dissolution at elevated temperature (50–60 °C) and related capacity fade [1]. Various oxide coatings on the cathode material have been studied to eliminate these drawbacks or to improve the performance. For example, studies on  $\text{Li}_2\text{O}-\text{B}_2\text{O}_3$ -glass coating [2] and  $\text{LiCoO}_2$  coating [3] on  $\text{LiMn}_2\text{O}_4$  spinel material were reported to improve the performance of the spinel material at elevated temperature,  $\text{MgO}$  coatings on  $\text{LiNi}_{1-x}\text{M}_x\text{O}_2$  and its modified compounds [4,5] were also found to improve the performance of the material, although optimum improvement has yet to be achieved. Recently, similar studies of coatings have been

extended to the presently used  $\text{LiCoO}_2$  material to enhance its cycling performance. Various metal oxide coatings such as  $\text{Al}_2\text{O}_3$  [6–9],  $\text{ZrO}_2$  [6,9,10],  $\text{TiO}_2$  [6],  $\text{SnO}_2$  [11], and  $\text{MgO}$  [8] have been shown to improve both the cycle-life (especially at high-voltage charging) and the rate capability of the  $\text{LiCoO}_2$  cathode in coin-type half-cells. Nevertheless, the working mechanism is not well understood [6,10].

In this investigation, an examination is made of the beneficial effects of  $\text{Al}_2\text{O}_3$  and  $\text{MgO}$  coatings on  $\text{LiCoO}_2$  cathode material with respect to the thermal stability of the material and the electrical and safety performance of 18650-size Li-ion cells.

### 2. Experiment

$\text{MgO}$  coating of  $\text{LiCoO}_2$  cathode material was performed by treating commercial  $\text{LiCoO}_2$  powder with a 5% methanol solution of Mg methoxide. Solution-wet powder was dried and then heat treated at temperatures between 500 and 800 °C in air for 10 h. After cooling, the powder was sieved through a 325 mesh screen to filter out lumps. All samples of cathode material including the uncoated control sample, were dried at 120 °C overnight or longer.  $\text{Al}_2\text{O}_3$  coating of  $\text{LiCoO}_2$  cathode material was conducted in a similar fashion by treating commercial  $\text{LiCoO}_2$  powder with a 5% ethanol solution of Al-isopropoxide. The heat-treatment temperature

\* Corresponding author. Tel.: +82-31-288-4570; fax: +82-31-288-4504.  
E-mail address: [hojin.kweon@samsung.com](mailto:hojin.kweon@samsung.com) (H.-J. Kweon).

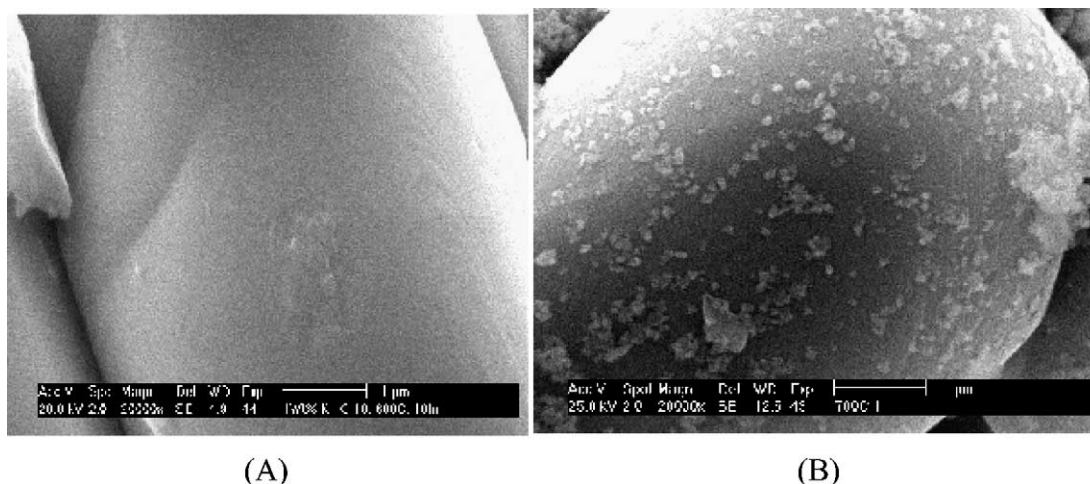


Fig. 1. Electron micrograph of  $\text{LiCoO}_2$  powder: (A) uncoated particle; (B)  $\text{Al}_2\text{O}_3$  coated particle.

was between 300 and 700 °C. A typical content of Al or Mg in the coated powder was 1–2 at.% of cobalt. Scanning electron microscopic (SEM; Philips, XL30) images of the surface morphology of the  $\text{Al}_2\text{O}_3$  coating are shown in Fig. 1.

The sample cathode was prepared by coating an Al foil with a *N*-methyl-2-pyrrolidone (NMP) slurry which contained 94 parts of the cathode material, 3 parts of Super P-carbon black (MMM Company), and 3 parts of polyvinylidene fluoride (PVdF) binder material. After drying at 130 °C for 1 h the material was compressed to desired thickness with a rolling press and cut into the test electrodes. The coin-type test cells (size 2016) used in this study were composed of a sample cathode, a Li metal anode, a sheet of micro-porous polyethylene separator, and an electrolyte of 1 M  $\text{LiPF}_6$  solution in 1:1 (by volume) mixture of ethylene carbonate (EC) and dimethyl carbonate (DMC). Lithium was used for counter and reference electrodes. All cells, after addition of the electrolyte, were aged at room temperature for 24 h prior to the electrochemical tests. The Li-ion cells were of the 18650-type wound cylindrical design and had a nominal capacity of 2000 mAh. An uncoated or an  $\text{Al}_2\text{O}_3$  coated  $\text{LiCoO}_2$  powder served as the cathode material, and the electrolyte was a multi-component carbonate based solution with  $\text{LiPF}_6$  salt.

X-ray diffraction (XRD) studies were carried out using a X-ray diffractometer (Philips PW 1340; Cu  $\text{K}\alpha$ ). Secondary ion mass spectroscopy (SIMS) and X-ray photoelectron spectroscopy (XPS) studies were performed with SIMS equipment made by VG Scientific (~10 keV; depth of resolution = tens of nm; atomic detection limit of a few ppm) and Model PHI 5600 (PHI) XPS equipment, respectively.

Capacity measurements and cycling tests of the coin-type cells were carried out between 2.75 and 4.3 V at 0.1–1 C rates of charge and discharge using Toyo multi-channel cyclers with an accuracy of 0.5% or better for charge/discharge currents. The 1 C rate was equivalent to 140 mA  $\text{g}^{-1}$ . Cycle-life

tests of the coin cells were carried out with a 4.3 V charge cut-off. The cells were subjected to 1 cycle at the 0.1 C rate, 3 cycles at the 0.2 C rate, and 10 cycles at the 0.5 C followed by continuous cycling at the 1 C rate. Previous results had indicated that the coin cell capacity was not limited by the Li metal counter electrode for at least 80 cycles in a cycling condition similar to that used in this study. The 18650 cells were cycled by charging at a constant current at the 1 C rate to a voltage cut-off of 4.2 V, followed by float charging at the cut-off voltage for total charge time of 2.5 h.

Samples for differential scanning calorimetry (DSC) were prepared by disassembling charged coin cells (to 4.3 V at 0.1 C rate) in a glove box, removing the charged cathode, and cutting out the DSC sample in an appropriate size. All sample electrodes contained 30–35 wt.% of electrolyte with respect to the dry cathode. Approximately 10 mg of the cathode containing the electrolyte was hermetically sealed in an aluminium DSC sample pan. Active material only was considered for the calculation of the heat flow. All experiments were performed at a heating rate of 3 °C/min using a TG-DTA/DSC (Setaram, France) apparatus.

### 3. Results and discussion

#### 3.1. Physical characterization of MgO and $\text{Al}_2\text{O}_3$ coated $\text{LiCoO}_2$

**XRD results:** The XRD patterns of MgO and  $\text{Al}_2\text{O}_3$  coated  $\text{LiCoO}_2$  cathode materials with heat treatment at various temperatures are shown in Fig. 2. The patterns remain basically unchanged after oxide coating and heat treatment up to 800 °C, which suggests that the coating has modified only the surface of the active material without changing the crystal structure of the bulk active material.

**SIMS and XPS results:** The Mg and Al distribution profiles into the depth of  $\text{LiCoO}_2$  particles from the surface,

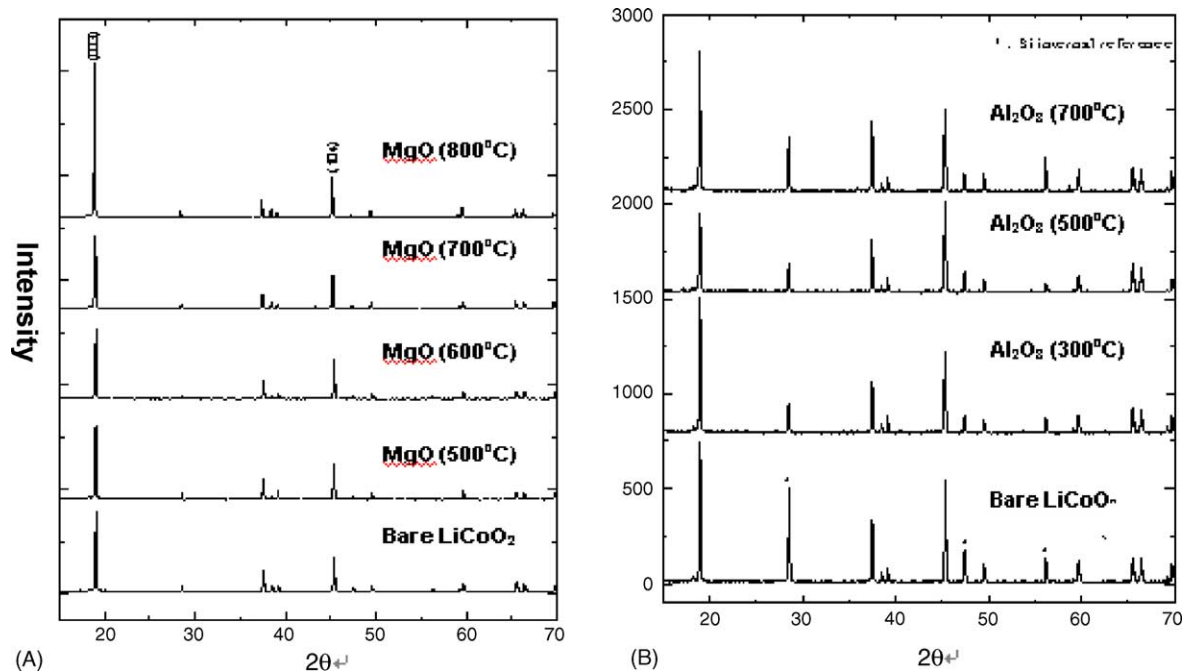


Fig. 2. XRD patterns of bare (uncoated) and MgO and Al<sub>2</sub>O<sub>3</sub> coated LiCoO<sub>2</sub> powder at various temperatures: (A) bare and Mg coated powder samples at 500, 600, 700 and 800 °C; (B) bare and Al<sub>2</sub>O coated powder at 300, 500 and 700 °C.

as determined by SIMS, are shown in Fig. 3. The curves show that the concentrations of Mg and Al decrease as the sputtering time increases while, uncoated powder does not indicate the presence of Al. This suggests that the coating element (Mg or Al) is present only at the surface of the active material. XPS analysis (not shown) of an Al-coated powder sample agreed qualitatively with the SIMS results.

### 3.2. Effect of coating on electrochemical properties

Typical initial charge and discharge curves of cathodes of uncoated and Al<sub>2</sub>O<sub>3</sub> coated LiCoO<sub>2</sub> in a coin-type cell that contains a 1 M LiPF<sub>6</sub>-EC/DMC (1:1) electrolyte are shown in Fig. 4. These curves show that the cathode polarization for both charge and discharge is reduced substantially by the Al<sub>2</sub>O<sub>3</sub> coating, as indicated by the magnitude of the voltage

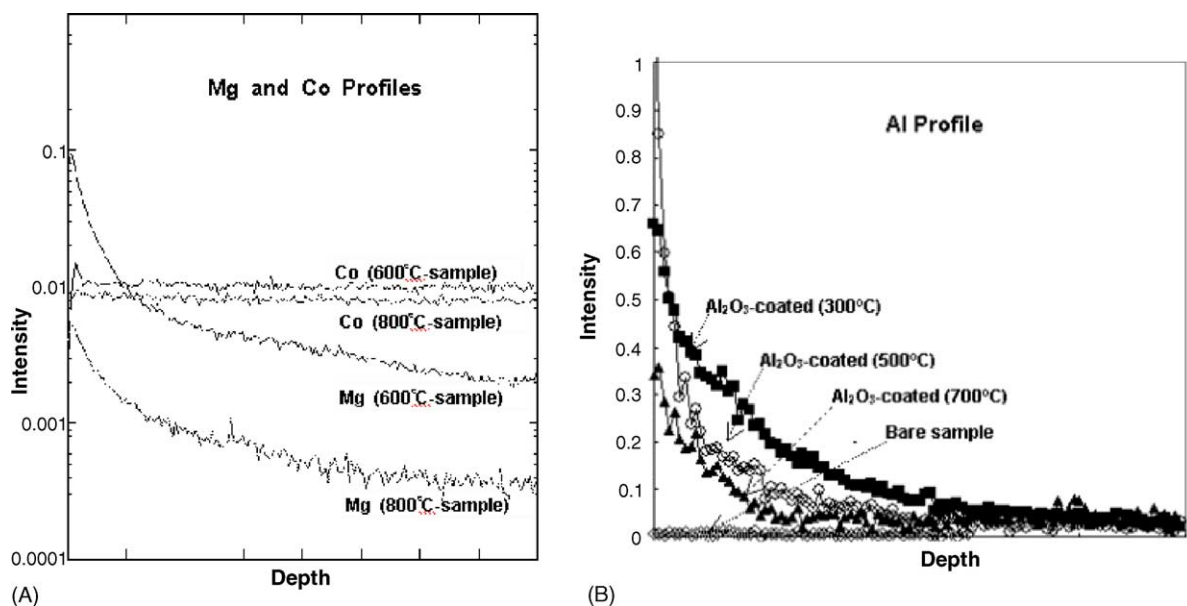


Fig. 3. SIMS elemental-concentration-depth profiles of MgO and Al<sub>2</sub>O<sub>3</sub> coated LiCoO<sub>2</sub> powder particles: (A) Mg and Co profiles in MgO coated samples heat reacted at 600 and 800 °C, respectively; (B) Al profiles in Al<sub>2</sub>O<sub>3</sub> coated samples heat treated at 300, 500 and 700 °C, respectively, and a bare sample.

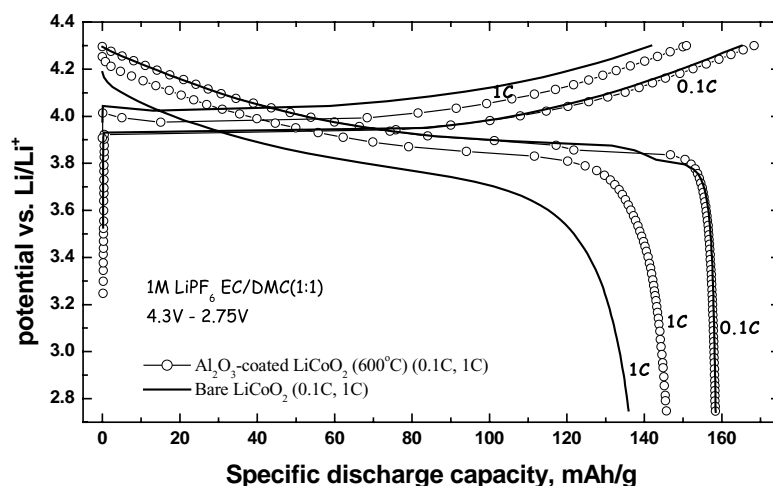


Fig. 4. Typical charge and discharge voltage curves of bare and  $\text{Al}_2\text{O}_3$  coated  $\text{LiCoO}_2$  cathodes in 1M  $\text{LiPF}_6$ -EC/DMC (1:1) electrolyte.

changes between curves at 0.1 and 1 C rates. The discharge capacity at high rate (1 C) is also improved by the coating. These results suggest that the rate capability of the electrode is improved substantially by the coating. The  $\text{MgO}$  coating also produces similar beneficial effects, although the effects are slightly less pronounced than those found with the  $\text{Al}_2\text{O}_3$  coating.

The cycle-life of the electrode is also substantially improved by the oxide coatings, as shown in Fig. 5. The data indicate that retention of cathode capacity on cycling is improved by both  $\text{MgO}$  and  $\text{Al}_2\text{O}_3$  coatings, but that the latter coating is slightly more effective. These findings are in good agreement with those of our earlier studies [4,12] as well as those reported by others [9,13,14]. The present results do not, however, show a conclusive trend on the effects of heat-treatment temperature of the  $\text{Al}_2\text{O}_3$  coating in the range of 300–700 °C, although there is a tendency that treat-

ment at 300 °C appears to cause better capacity retention than observed with the use of higher temperatures.

### 3.3. Effect of coating on the thermal stability

The DSC curves for fully-charged  $\text{MgO}$  and  $\text{Al}_2\text{O}_3$  coated  $\text{LiCoO}_2$  active material, without removing the electrolyte, are compared with that of corresponding uncoated material in Figs. 6 and 7, respectively. The onset temperature for thermal decomposition is raised significantly and the total amount of the reaction heat is reduced by both  $\text{MgO}$  and  $\text{Al}_2\text{O}_3$  coatings. The onset temperature of the  $\text{MgO}$  coated material is sensitive to the heat-treatment temperature, as shown in Fig. 6. At present, however, the reason for such sensitivity is not well understood. Although a quantitative relationship between the DSC data and actual safety characteristics of the Li-ion cells is not available, the present results

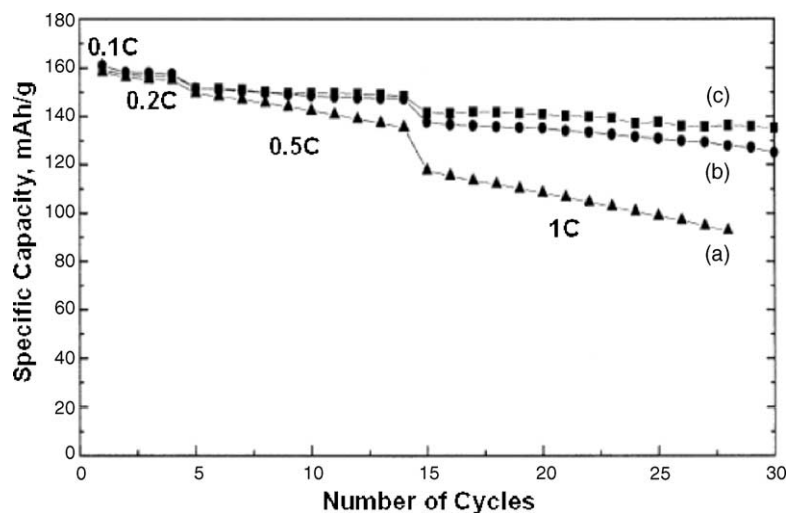


Fig. 5. Specific capacity changes on cycling of  $\text{LiCoO}_2$  active material: (a) bare; (b)  $\text{MgO}$  coated with heat treatment at 700 °C; (c)  $\text{Al}_2\text{O}_3$  coated with heat treatment at 600 °C.

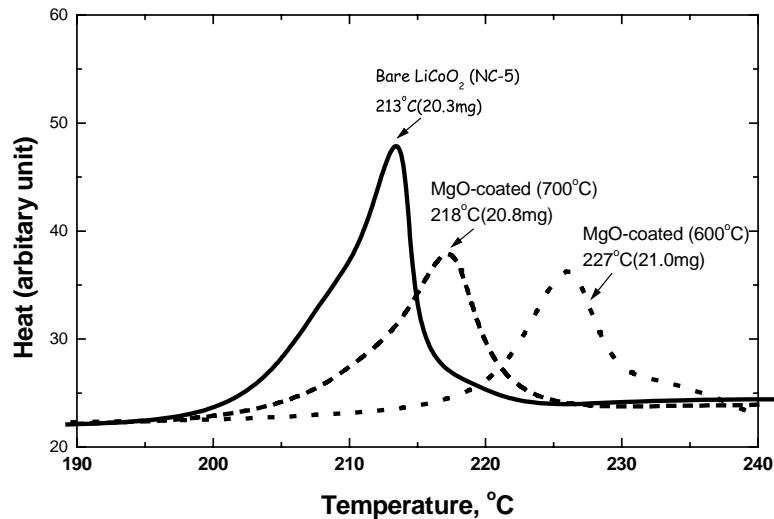


Fig. 6. DSC curves of fully-charged MgO coated LiCoO<sub>2</sub> active material with heat treatment at 600 and 700 °C and corresponding uncoated material.

suggest that the safety of charged Li-ion cells is definitely improved when the active material is coated with either one of the oxides.

### 3.4. Electrical performance in 18650-type Li-ion cells

The average charge and discharge voltage curves at the 1 C rate of five 2000 mAh 18650-size cylindrical Li-ion cells that contain an Al<sub>2</sub>O<sub>3</sub> coated LiCoO<sub>2</sub> cathode material and the corresponding uncoated material for control are shown in Figs. 8 and 9, respectively, for cycles 1, 100, 200 and 300. The corresponding discharge capacities are plotted against cycle number in Fig. 10.

The charge-acceptance values for the first-cycle charge of the two different types of cells are more or less similar. The control cells containing uncoated material accepted charge to approximately 74% of the nominal capacity, whereas cells containing the coated material accept 78%. On the other hand, charge-acceptance of the control cell decreases rapidly

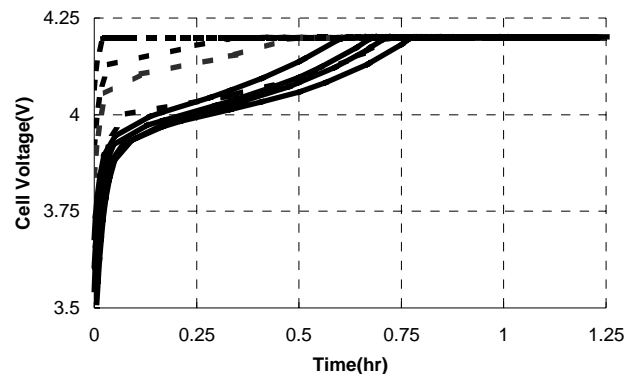


Fig. 8. Charge voltage curves of 18650-size Li-ion cells (nominal 2000 mAh) containing uncoated and Al<sub>2</sub>O<sub>3</sub> coated LiCoO<sub>2</sub> cathodes. Dotted line curves are for uncoated material and solid for coated material. The curves from bottom to top are for cycles 1, 100, 200 and 300, respectively. Cells were charged at 1 C rate to 4.2 V followed by a constant voltage charge at this voltage for a total charge time of 2.5 h and discharged at 1 C rate to 2.75 V.

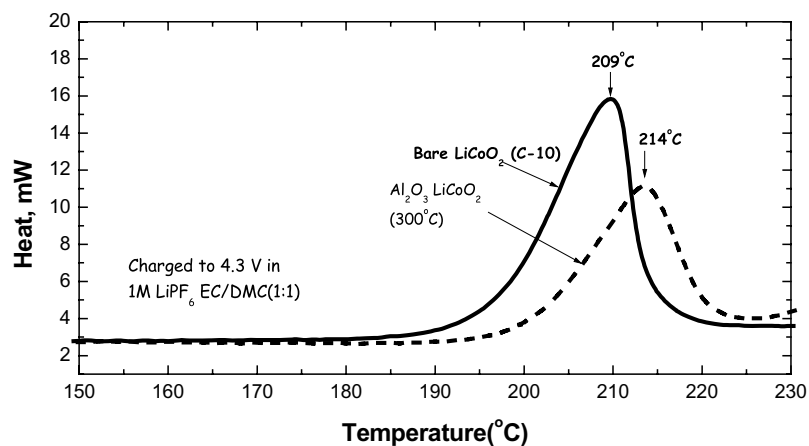


Fig. 7. DSC curves of fully-charged Al<sub>2</sub>O<sub>3</sub> coated LiCoO<sub>2</sub> active material with heat treatment at 300 °C and corresponding uncoated material.

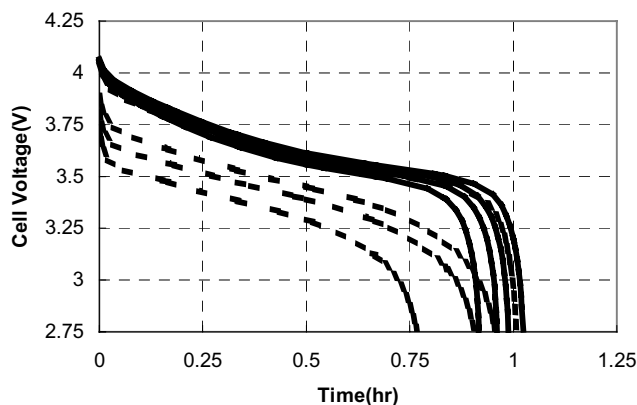


Fig. 9. Corresponding discharge curves to the charge curves shown in Fig. 10. Dotted lines curves are for uncoated material and solid for coated material. The curves from top to bottom are for cycles 1, 100, 200 and 300, respectively.

with cycling, while that of the cell with coated material exhibits minimal decrease. The 1 C-rate charge-acceptance of the control cell is approximately 50, 35 and 3% at cycles 100, 200 and 300, respectively. By contrast, that of the cell with coated material is as high as 60% even after 300 cycles.

The results also show that the charge and discharge voltages of cells containing the  $\text{Al}_2\text{O}_3$  coated material are relatively unchanged with the cycling, whereas the charge and discharge voltages of the control cells deteriorate rapidly, as shown in Figs. 8 and 9. This indicates that the internal impedance of a cell containing the  $\text{Al}_2\text{O}_3$  coated material is lower and much more stable on cycling than that of the control cell.

The control cell and those containing the coated material display comparable discharge capacities of 2017 and 2048 mAh, respectively, for the first cycle. Nevertheless, the discharge capacity of the control cell decreases rather rapidly with cycling, while that of the cells with coated material give much improved capacity retention, as shown in Fig. 10. The capacity decrease after 300 cycles is 22 and 11% for these two different cell types, respectively. Overall, it is concluded

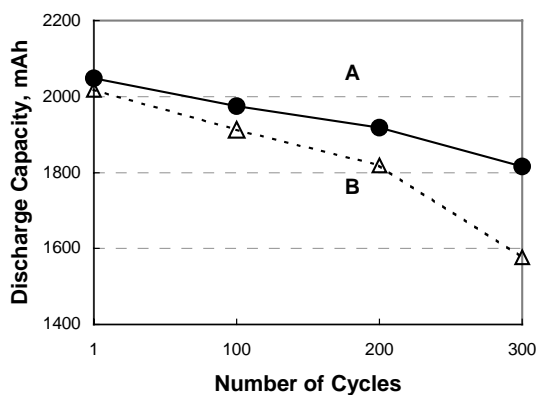


Fig. 10. Discharge capacity of 18650 cells (nominal 2000 mAh) containing: (A)  $\text{Al}_2\text{O}_3$  coated  $\text{LiCoO}_2$  active material; (B) uncoated material as function of cycle number.

Table 1  
Summary of safety tests of 18650 Li-ion cells

Test item	Uncoated $\text{LiCoO}_2^a$	$\text{Al}_2\text{O}_3$ coated <sup>a</sup>
Overcharge (1 C to 12 V)	All fail (10)	Eight pass
Heat exposure (charged/50 °C)	All fail (5)	Four pass; one fail
Overcharge penetration (4.35 V)	All fail (5)	Four pass
Compression (fully charged)	All fail (5)	Seven pass; one fail
Collision (fully charged)	All fail (8)	Eight pass

<sup>a</sup> Numbers in parentheses represent number of test cells. 'Fail' represents flame or explosion and 'pass' no flame.

that an  $\text{Al}_2\text{O}_3$  coating on the  $\text{LiCoO}_2$  cathode material substantially improves the charge and discharge rate capability and cycle-life of Li-ion cells.

### 3.5. Safety performance of 18650-type Li-ion cells

A series of preliminary safety tests was carried out on 2000 mAh 18650 Li-ion cells which contained uncoated or  $\text{Al}_2\text{O}_3$  coated  $\text{LiCoO}_2$  cathode material. These tests included overcharge to 12 V at the 1 C rate, heat exposure at 150 °C for 10 min, nail penetration of an overcharged cell to 4.3 V, mechanical impact and crush tests of charged cells. The results of these tests are summarized in Table 1, and clearly indicate that the safety characteristics of 18650 Li-ion cells are improved remarkably by the  $\text{Al}_2\text{O}_3$  coating, which is in qualitative agreement with DSC results.

### 3.6. Possible mechanisms

Two different mechanisms have been suggested previously for the improvement in cycle-life of cathode material by metal oxide coatings. Cho et al. [6] reported that the crystallographic deformation of  $\text{LiCoO}_2$  during charge and discharge is reduced rather drastically in the presence of a  $\text{Al}_2\text{O}_3$  or a  $\text{ZrO}_2$  coating. This conclusion was reached from XRD studies of electrodes containing uncoated and coated  $\text{LiCoO}_2$  at various states-of-charge in an ex situ condition [6]. Later, for an in situ condition in a cell, Chen and Dahn [10] could not observe any change in the crystallographic deformation of  $\text{LiCoO}_2$  with a  $\text{ZrO}_2$  coating [10]. They suggested that the improvement in cycle-life may simply be due to a reduced contact area of the charged active material with the electrolyte by the  $\text{ZrO}_2$  coating. This simple mechanism may explain the extended cycle-life and the improvement of safety characteristics but it cannot explain the observed improvement in the rate capability that is caused by the coating. In same way, the metal oxide coating must improve the  $\text{Li}^+$ -ion conductivity through the electrolyte-active material interface. Therefore, it is speculated that the  $\text{Al}_2\text{O}_3$  coating provides the interface with a chemically stable, but highly  $\text{Li}^+$ -ion conductive, barrier layer that effectively reduces the chemical reaction between the charged active material and the electrolyte such that it gives good rate capability, long cycle-life, and good safety characteristics. It is also con-

cluded that the barrier layer might be in the form of a composite of nano-particles of  $\text{Al}_2\text{O}_3$  and an organic product of a reaction between the electrolyte and charged active material.

#### 4. Conclusion

$\text{Al}_2\text{O}_3$  and  $\text{MgO}$  coatings (especially the former) on  $\text{LiCoO}_2$  cathode active material induce substantially beneficial effects on Li-ion cell. These effects include greatly improved charge and discharge rate capability, increased cycle-life, and greater safety characteristics. The enhanced cycle-life includes good retention of both capacity and rate capability.

#### References

- [1] J.-M. Tarascon, M. Armand, *Nature* 414 (2001) 359.
- [2] G.O. Amatucci, A. Blyr, C. Sigala, P. Alfonse, J.-M. Tarascon, *Solid State Ionics* 104 (1997) 13.
- [3] J. Cho, O.B. Kim, H.S. Lim, C.-S. Kim, S.-I. Yoo, *Electrochem. Solid-State Lett.* 2 (1999) 607.
- [4] H.-J. Kweon, D.G. Park, *Electrochem. Solid-State Lett.* 3 (2000) 128.
- [5] H.-J. Kweon, S.J. Kim, D.G. Park, *J. Power Sources* 88 (2000) 255.
- [6] J. Cho, Y.J. Kim, T.-J. Kim, B. Park, *Angew. Chem. Int. Ed.* 40 (2001) 3367.
- [7] Y.J. Kim, T.-J. Kim, J.W. Shin, B. Park, J. Cho, *J. Electrochem. Soc.* 149 (2002) 1337.
- [8] Z. Wang, L. Liu, L. Chen, X. Huang, *Solid State Ionics* 148 (2002) 335.
- [9] A.M. Kannan, L. Rabenberg, A. Manthiram, *Electrochem. Solid-State Lett.* 6 (2003) A16.
- [10] Z. Chen, J.R. Dahn, *Electrochem. Solid-State Lett.* 5 (2002) 213.
- [11] J. Cho, C.-S. Kim, S.-I. Yoo, *Electrochem. Solid-State Lett.* 3 (2000) 362.
- [12] J. Cho, Y.J. Kim, B. Park, *Chem. Mater.* 12 (2000) 3788.
- [13] L. Liu, Z. Wang, H. Li, L. Chen, X. Huang, *Solid State Ionics* 152-3 (2002) 341.
- [14] Z. Wang, C. Wu, L. Liu, F. Wu, L. Chen, X. Huang, *J. Electrochem. Soc.* 149 (2002) A466.